An Electromechanical Model of the Heart for Image Analysis and Simulation

M. Sermesant

Ph.D Thesis Summary

Supervised by Nicholas Ayache and Hervé Delingette

Publicly Defended on the 26th of May 2003

Jury:

Michel Barlaud, CNRS

Isabelle Magnin, INSA Creatis

Derek Hill, King's College London

Frédérique Clément, INRIA

Olivier Gérard, Philips Medical Systems

Hervé Delingette, INRIA

Nicholas Ayache, INRIA

Research done in the Epidaure Research Project, INRIA Sophia Antipolis

Abstract

This Ph.D thesis presents a dynamic model of the cardiac electromechanical activity for the analysis of time series of medical images and the simulation of the cardiac function. First, a method to build volumetric biomechanical models based on tetrahedral meshes is presented. Then, the action potential propagation is simulated using FitzHugh-Nagumo reaction-diffusion equations, enabling the introduction of pathologies and the simulation of surgical procedures. The myocardium contraction is modelled according to a rheological law which includes an electromechanical coupling and boundary conditions based on blood pressure and volume constraints.

Simulation of a cardiac cycle leads to the validation of some global and local cardiac function parameters. A cardiac image segmentation process integrating this electromechanical model is then introduced following the deformable model framework. Preliminary results of this segmentation system indicates that using *a priori* knowledge about the anatomy, mechanical behaviour and motion in a pro-active deformable model improves the robustness and accuracy of the segmentation despite the sparse and noisy nature of medical images.

keywords: heart, electro-mechanical model, deformable model, 4D cardiac images, action potential, electromechanical coupling, organ simulation

1 Introduction

New perspectives in medical image analysis and medical simulation are opened with the integration of knowledge from biology, physics and computer science. It makes possible to combine *in vivo* observation, *in vitro* experiments and *in silico* simulations.

From these three points of view, knowledge of the heart function has greatly improved at the nanoscopic, microscopic and mesoscopic scales during the last decade. Thus a global integrative work of this organ becomes conceivable [22].

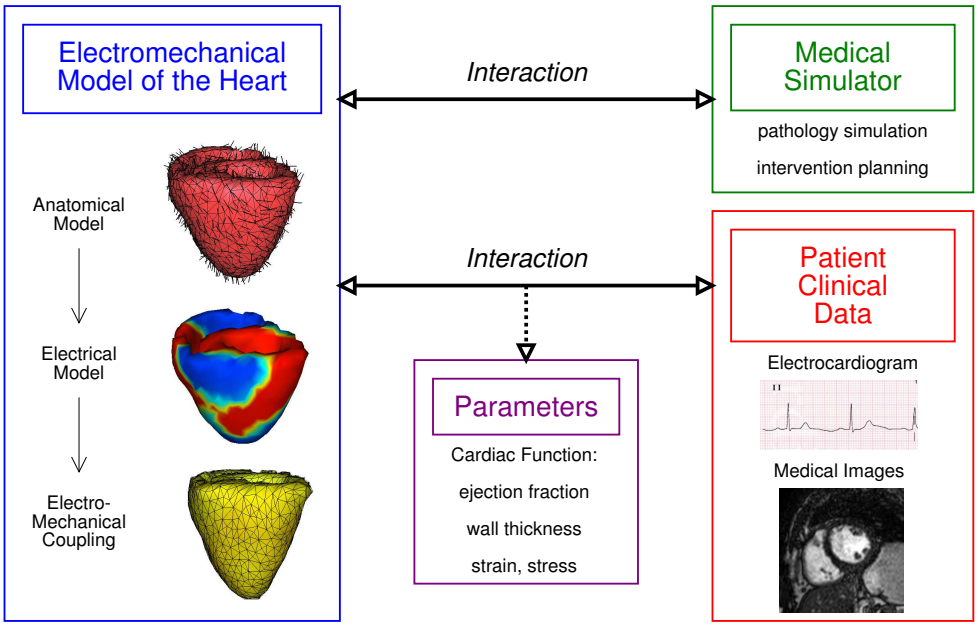

Figure 1: Overview of the presented work: electromechanical model construction, simulation of cardiac activity and clinical data analysis.

The clinical motivation of this Ph.D is the quantitative measurement of important ventricular function parameters from cardiac images, like the ejection fraction, the myocardium thickness and the local strain and stress. Those parameters are useful to detect ischemic zones, to measure the pathology extent and to control the therapy effectiveness.

The key idea is to build a "Pro-Active Deformable Model" of the heart. It is a volumetric deformable model of the heart integrating *a priori* knowledge on the motion, through the simulation of the electromechanical contraction.

Using a model with physics- and physiology-based parameters makes it also possible to simulate some cardiovascular pathologies and interventions. Current electrophysiology studies procedures are often lengthy due to the inner difficulties of x-rays, being a projection modality where soft tissues are not visible and the understanding of the measured electrograms in the context of patient anatomy can be difficult. This results in prolonged x-ray dose to the patient and the staff carrying out these procedures. Moreover, there is no certain way to predict the outcome of interventions such as radio frequency ablation or pacing. Such models could help devise a technique to make electrophysiology studies to correct abnormal heart rhythms less invasive and more successful.

The electro-mechanical model of the heart presented is based on mathematical systems of non-linear partial differential equations, set on a three dimensional domain, considering the ventricles as a continuum.

2 Anatomical Model

The myocardium is represented as a tetrahedral volumetric mesh including anatomical information. The process to build such a model is detailed in [34]. The main anatomical information used are the myocardium geometry, the location of different anatomical parts and muscle fibre directions.

2.1 Volumetric Mesh Creation

The geometry can be extracted from different medical image modalities. From a 3D image of the heart, the myocardium is segmented, using classical image processing methods like thresholding and mathematical morphology. Then, a triangulated surface of the myocardium is obtained using the marching cubes method [20], and it is decimated to the required size. Finally, a volumetric tetrahedral mesh is created from the triangulated shell, using the INRIA software GHS3D[1].

2.2 Anatomical Labelling of the Mesh

Then, to better control and analyse the model during the simulation, we label the anatomical mesh into different zones, corresponding to the ones defined in the myocardium atlas of the Visible Human Project [30]. This is done by registering the mesh with the atlas image, and then labelling each tetrahedron a class according to the voxels where centres are inside this tetrahedron (these voxels are obtained by rasterization, the whole procedure is detailed in [34]).

Fig. 3 presents the result of the anatomical regions attribution from the atlas to the mesh.

[1] `http://www-rocq.inria.fr/gamma/ghs3d/ghs.html`

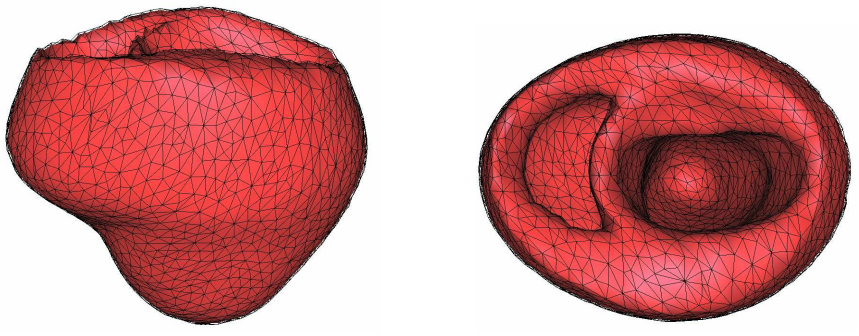

Figure 2: Tetrahedral mesh of the bi-ventricular myocardium (40 000 elements).

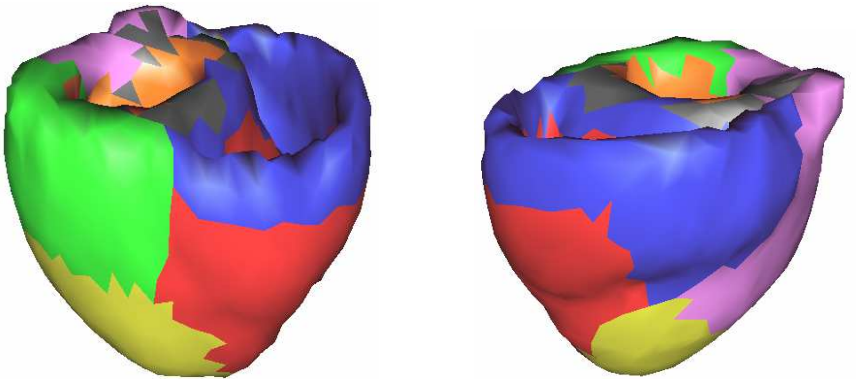

Figure 3: Anatomical regions obtained from the Visible Human atlas: Basal Left Endocardial Ventricle (orange), Basal Septum (grey), Dorsobasal Left Epicardial Ventricle (green), Basal Right Ventricle (blue), Basal Left Epicardial Ventricle (violet), Apical Right Ventricle (red), Apical Left Epicardial Ventricle (yellow).

2.3 Muscle Fibre Directions

The muscle fibre directions can be obtained from dissection measures or diffusion tensor MR images (DTI) [15]. We present in this article the model built from the dissection measures performed on a canine heart in the bioengineering lab of the Auckland University, New Zealand[2]. This dataset has been interpolated and smoothed by the bioengineering lab of the University of California, San Diego[3] [26].

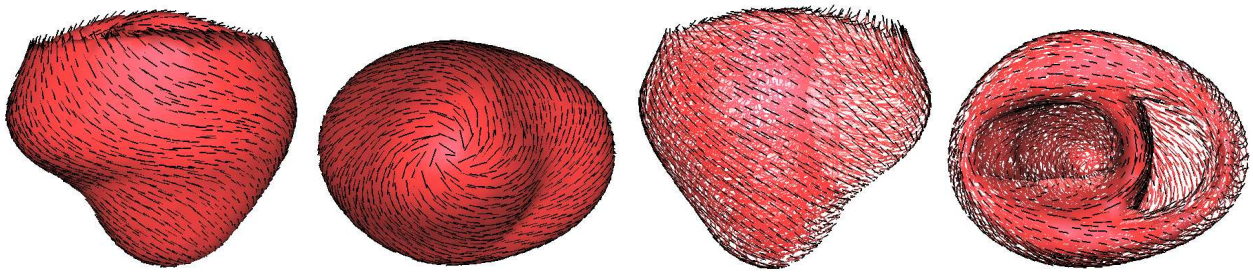

Figure 4: Fibre directions assigned to the myocardium mesh from the data interpolated in UCSD.

[2] http://www.bioeng.auckland.ac.nz/home/home.php

[3] http://cmrg.ucsd.edu/

These fibre directions are used in three components of the model:

- for the electrical action potential propagation, it represents a preferential propagation directions, through an anisotropic diffusion tensor (D)
- in the passive elastic element of the mechanical constitutive law, it represents the transverse anisotropy direction
- in the contractile element of the mechanical constitutive law, it gives the direction of the contraction stress

3 Electrical Model

Different models can be used to simulate the cardiac electrophysiology. The two main approaches are:

- a cellular level simulation, using as variables all the concentrations of the different types of ions, and integrating different ion channels [14, 4, 21, 27].
- a more macroscopic view using a simpler system of equations only computing the extra-cellular and intra-cellular potentials (or their difference, the action potential) [10, 1, 19].

As we model the electrophysiology to control the contraction, we use the latter approach, because the contraction is simply related to the action potential. Moreover, for clinical use, the extra-cellular potential can be measured, but not the different ions concentrations, so we could not adjust the models of the former approach.

3.1 Action Potential Simulation

The action potential wave propagation is simulated using a system based on FitzHugh-Nagumo equations. Such models yields fast 3D computations and the principal biological phenomena are well captured:

- a cell is activated only for a stimulus larger than a certain threshold;
- the shape of the action potential does not depend on the stimulus;
- there is a refractory period during which the cell cannot be excited;
- a cell can act as a pacemaker.

Aliev and Panfilov developed a modified version of the FitzHugh-Nagumo equations adapted to the dynamic of the cardiac electrical potential [1]. This model is further simplified, as the complete ε term is mainly useful to model the influence of changes in pacing frequency and this property is not needed at the moment. Here is the set of differential equation studied:

$$\begin{aligned} \partial_t u &= \operatorname{div}(D\,\nabla u) + ku(1-u)(u-a) - uz \\ \partial_t z &= -\varepsilon(ku(u-a-1)+z)) \end{aligned} \tag{1}$$

u is a normalised action potential and z is a secondary variable for the repolarisation. k and ε control the repolarisation, and a the reaction phenomenon. Parameters values are derived from [1]: $\varepsilon = 0.01$, $k = 8$, $a = 0.15$.

And the fibre directions intervene in the diffusion tensor D, which writes:

$$D = d_0 \begin{pmatrix} 1 & 0 & 0 \\ 0 & r & 0 \\ 0 & 0 & r \end{pmatrix}$$

in an orthonormal basis which first vector is in the local fibre direction. d_0 represents the longitudinal conductivity, and r the anisotropy ratio in the other directions. Action potential propagates twice as fast in the fibre direction than in the orthogonal directions, so, as the square of the speed is related to the conductivity, we use $r = 0.25$ (and $d_0 = 1.0$ in the normal case).

With an excitation above the initialisation threshold, the simulated action potential with this system is rather similar to measurements of cardiac action potentials (fig. 5).

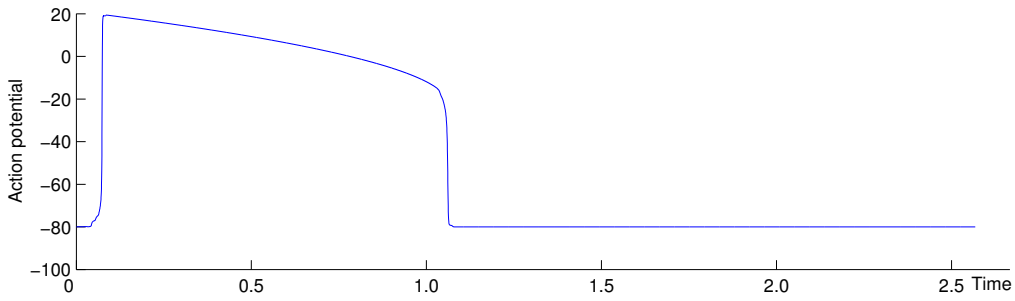

Figure 5: 1D measure of action potential simulation with simplified Aliev and Panfilov model.

3.2 Comparison of 3D Simulations with Available Measures

For a 3D simulation, we need to locate the electrical onset, namely the Purkinje network extremities, but it is hardly visible by dissection and by imaging. So we used the measures from Durrer *et al.* [8] to locate the Purkinje network extremities on the endocardia of both left and right ventricles[4].

A first validation of the 3D computation consists in comparing the resulting action potential isochrones with the measures from Durrer *et al.* (see fig. 6). The temporal integration is done with a forth order Runge-Kutta scheme and the spatial integration is done with linear tetrahedral elements. The computation time step is 5.10^{-4} and a 3D simulation takes around half an hour on a standard PC with a 40 000 elements tetrahedral mesh.

We also used invasive electrophysiological measures on canine hearts from the NIH, simulations along with measures comparison can be found in [33].

4 Electromechanical Model

The constitutive law used for the myocardium includes an active element controlled by the action potential computed in the previous section and a passive element representing the mechanical elasticity. Several constitutive laws have been proposed in the literature [18, 16,

[4]The color version presented here (fig. 6) was found on the web: `http://butler.cc.tut.fi/~malmivuo/bem/bembook/`

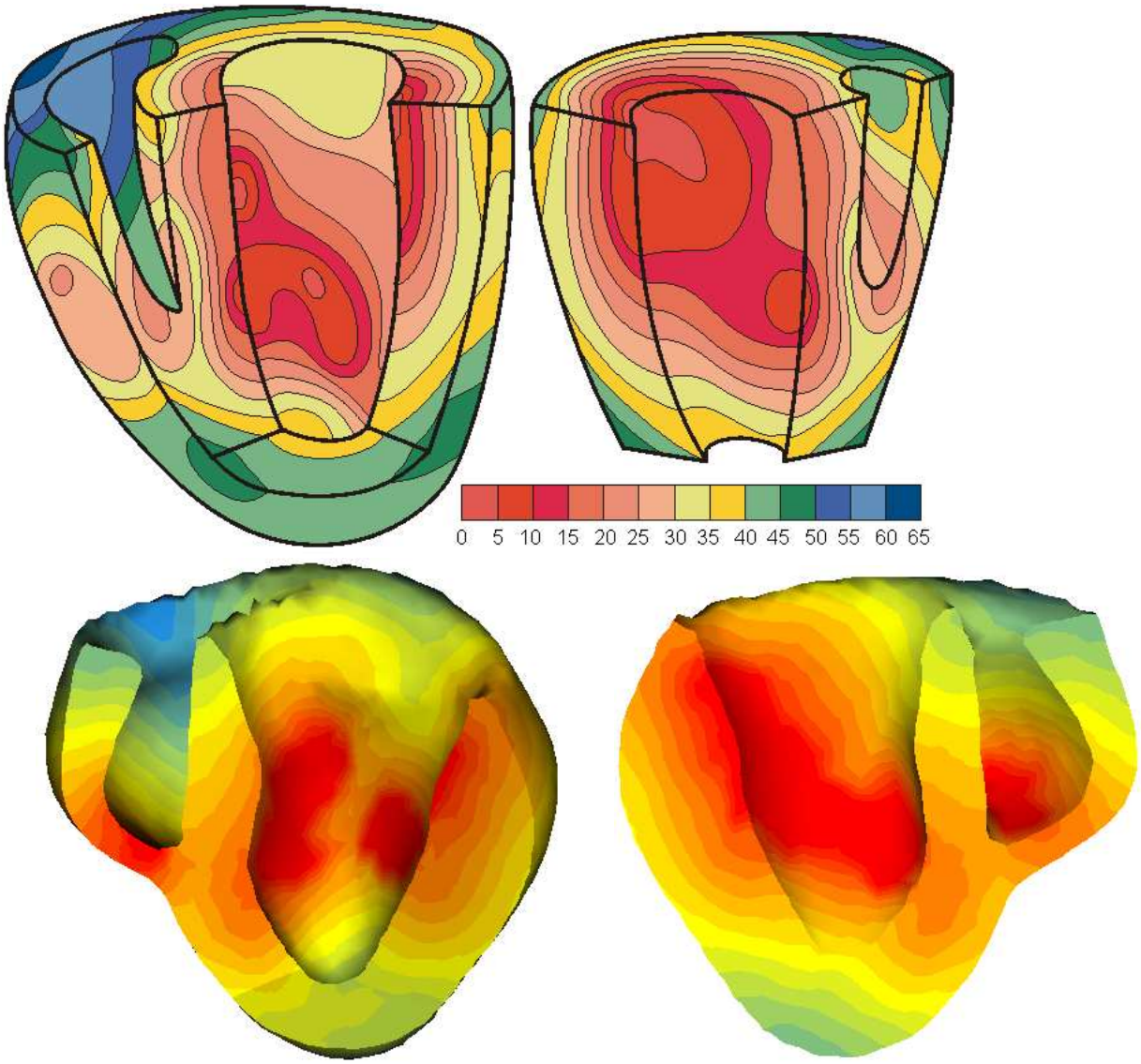

Figure 6: Action potential isochrones measured by Durrer *et al.* (top row) compared with the simulated ones using the model built from UCSD data (bottom row).

12, 17, 25, 13, 6], but currently none of them have been validated against clinical *in vivo* measures. The one presented below is based on the Bestel-Clément-Sorine model [5]:

$$\begin{cases} \rho\ddot{P} - \operatorname{div}(K_p\,\mathcal{E}_p + C_p\,\dot{\mathcal{E}}_p + \sigma_c + C_c\,\dot{\mathcal{E}}_c + K_c\xi_0) = 0 \\ \partial_t K_c = K_0|u|_+ - (|\dot{\mathcal{E}}_c| + |u|)K_c \\ \partial_t \sigma_c = \sigma_0|u|_+ - (|\dot{\mathcal{E}}_c| + |u|)\sigma_c + K_c\dot{\mathcal{E}}_c \\ \sigma_c + C_c\,\dot{\mathcal{E}}_c + K_c\xi_0 = K_s(\mathcal{E}_p - \mathcal{E}_c) \end{cases} \tag{2}$$

with P the position, K the stiffness, C the damping, $\mathcal{E}$ the strain, σ the stress, u the normalised action potential and X_c referring to the contractile element, X_p to the parallel element and X_s to the series element. This model fits into the Hill-Maxwell framework, with a contractile, a parallel and a series elements. A detailed study of this complete model along with 1-dimensional simulations can be found in [7].

The electromechanical model proposed is specifically designed for cardiac image analysis and simulation. It is built in order to be computationally efficient. We chose a simplified

constitutive law, as the image information can be used to correct the computed motion. Thus in this framework, the model can be directly compared with *in vivo* measures through medical images, thus making a validation possible. And despite its simplicity compared to other constitutive laws proposed in the literature, it reproduces quite well the behaviour of the myocardium.

The simplified mechanical model has the following components:

- a contractile element which creates a stress tensor σ_c
- a parallel element which is anisotropic linear visco-elastic and creates a stress tensor σ_p

For the electromechanical coupling, different laws have also been proposed [18, 25]. We chose a simple ordinary differential equation to control the coupling, directly computing the contraction intensity from the action potential. We believe that it is important to keep the model simple enough as not many measures are available to adjust this law. The contractile element is controlled by the electrical action potential through the ODE:

$$\partial_t \sigma_c = \sigma_0 |u|_+ - |u|\sigma_c$$

The tridimensionnal contraction stress tensor is obtained with the formula $\sigma_c f \otimes f$, where f denotes the fibre direction.

The behaviour of such a constitutive law is shown on a cube (see fig. 7). We can observe that the Lamé coefficients chosen to partly represent the incompressibility make the cube dilate vertically while it compresses horizontally.

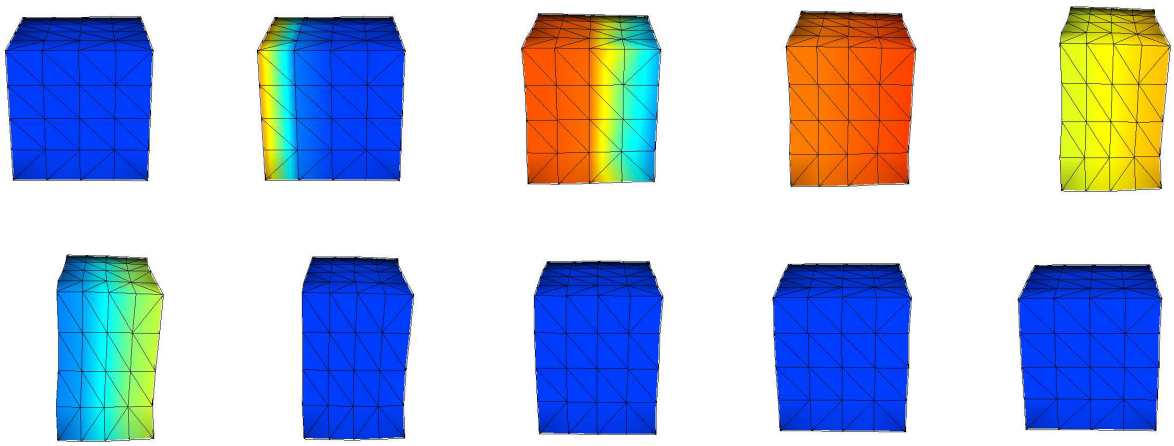

Figure 7: Contraction simulation (first row) then relaxation (second row) on a cube. Fibres are horizontal and a initial action potential is applied on the left face. Colours represent the normalised action potential value (blue: 0, red: 1).

To perform these electromechanical simulations, we solve the dynamics equation:

$$M\frac{d^2U}{dt^2} + C\frac{dU}{dt} + KU = F \tag{3}$$

with U the displacement vector, M the diagonal mass matrix (mass lumping), C the Rayleigh damping matrix, K the anisotropic (piecewise) linear elastic stiffness matrix and F the different loads, including the stress tensor from the contraction.

This equation is integrated in time using the Houbolt semi-implicit scheme, and in space using the Finite Element Method with tetrahedral linear elements. The implementation has been done using the PETSc[5] library for linear algebra operations, thus allowing parallel computations of the preconditioning and of the iterative solvers.

4.1 Complete Cardiac Cycle Simulation

To simulate an entire cardiac cycle, the interaction of the myocardium with the blood pool is very important. This is why the different phases of the cardiac cycle have been introduced, with different boundary conditions. The heart cycle can be divided in four phases:

- *Filling*: a pressure is applied to the vertices of the endocardium. Its intensity is equal to the mean pressure of the atrium;
- *Isovolumetric contraction*: a constraint is applied to the vertices of the endocardium, to keep the ventricle volume constant;
- *Ejection*: a pressure is applied to the vertices of the endocardium. Its intensity is equal to the mean pressure of the aorta (for the left ventricle) and the pulmonary artery (for the right ventricle);
- *Isovolumetric relaxation*: a constraint is applied to the vertices of the endocardium, keeping the volume constant.

We set the boundary conditions by introducing springs maintaining the basal nodes, to represent the fibrous structure around the valves.

In a first version, the succession of the different phases was triggered by a synchronisation mechanism based on a standard ECG, but it can also be automatically controlled by looking at the simulated pressure in the ventricles and comparing it to the simulated pressures in the atria and the arteries to trigger the opening and the closing of the different valves.

The pressure is estimated during the isovolumetric phases as the stress needed to keep the volume constant. For the other phases, the valves can close when the volume variation changes sign (the flow reverses). These more "natural" boundary conditions allow a better continuity in the stress and more realistic simulations.

The whole cardiac cycle simulation takes less than 30 minutes on a standard PC, half of this time is related to the isovolumetric phases since they require a very small time step for stability.

4.2 Simulated Cardiac Function Parameters

The simulation performed includes the propagation of the action potential in the myocardium, coupled with the mechanical contraction, using different boundary conditions depending of the phase of the cardiac cycle.

From this simulation of the cardiac cycle, different global and local parameters of the model can be observed. These parameters are compared with the ones extracted from tagged MRI by Philips Research France [2].

[5] `http://www-unix.mcs.anl.gov/petsc/petsc-2/index.html`

4.2.1 Volume of the Ventricles

We define a set of triangles representing the endocardium of each ventricle and we then close this surface to compute the volume of the ventricles (red surfaces and green lines in fig. 8). The evolution of these volumes during the simulation of the cardiac cycle is very similar to the one measured (fig. 8).

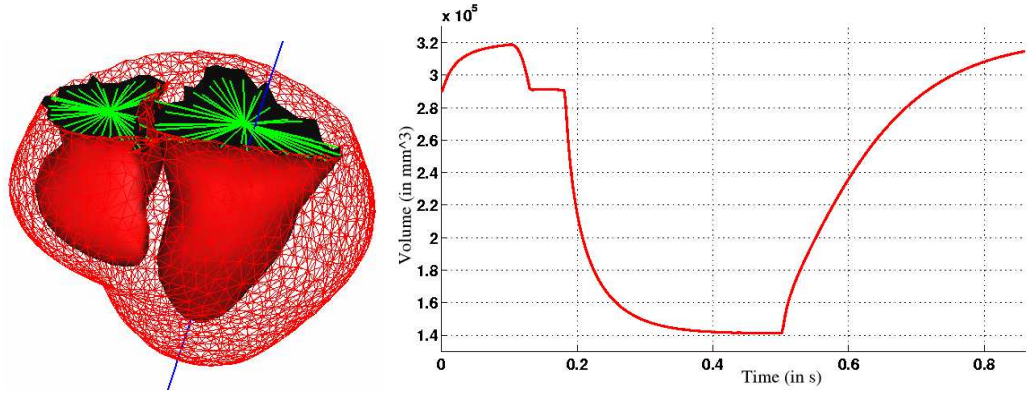

Figure 8: Left ventricle volume evolution during the simulated cycle. The values correspond to the volume in mm^3 of the data from Auckland, which should be scaled to obtain human range values. But the shape of the curve and the ejection fraction (56%) are similar to normal human data.

The evolution of these volumes allows to set the contractility parameter σ_0, that controls the maximum contraction, and thus is closely related to the ejection fraction.

4.2.2 Local Rotation

From the definition of the left ventricle endocardium, we can compute the inertia axis of the left ventricle (blue line in fig. 8). We use this axis to compute the local rotation of any point around this axis, along the cardiac cycle. The same rotation has been measured for different points of the myocardium by Philips Research France through the analysis of tagged MRIs [2].

By comparison with the model, the range of values is very similar between the simulation and the measures as well as the variation. And especially, the opposite direction rotation between the base and the apex is present both in the simulation and in the measures. This twisting motion originates from the fibre directions but also from the isovolumetric phase and the activation sequence. The simulation of the action potential propagation and of the different phases of the cardiac cycle is thus important to recover local parameters of the cardiac motion.

4.2.3 Local Radial Contraction

Another important local parameter of the cardiac function is the radial contraction, which measures the variation of the distance from any point to the central axis, along the cardiac cycle. The same inertia axis as for the rotation is used to compute the radial contraction of a point of the myocardium during the simulated cycle.

The comparison of the simulated radial contraction with the measured one gives also a good correlation, which confirms the fact that the simulated ejection fraction is close to the

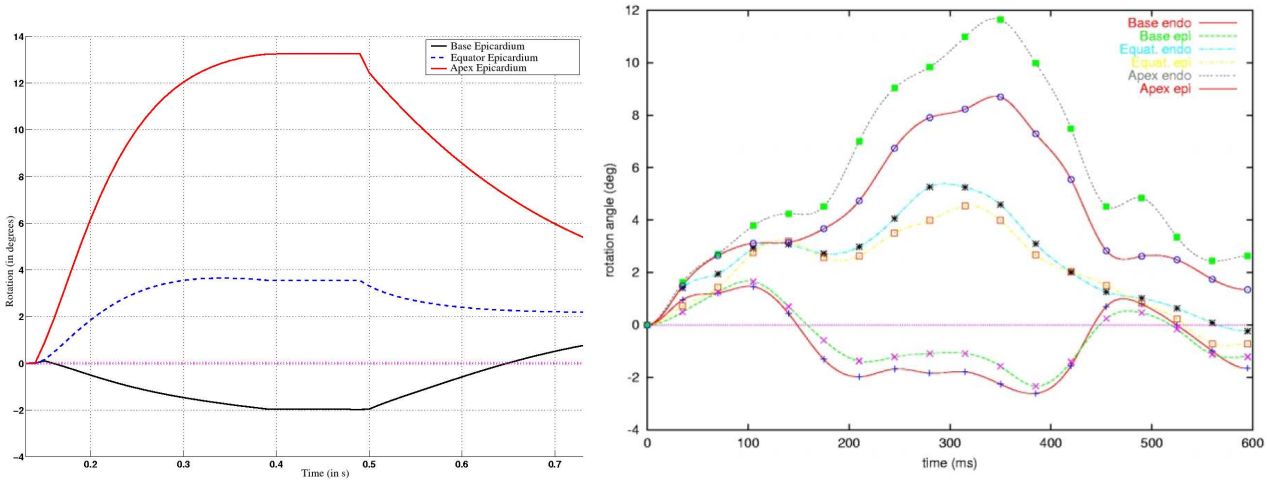

Figure 9: (Top) Twist angle during the simulated cycle, for different points of the epicardium: base (black), equator (blue - -) and apex (red). (Bottom) Twist angle extracted from tagged MRI by Philips Research France for different points of the myocardium.

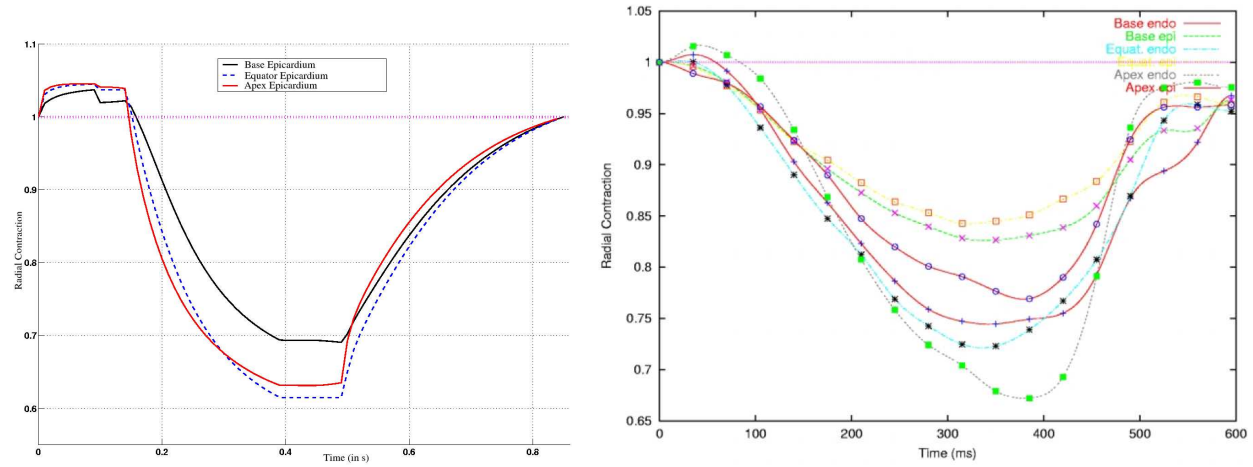

Figure 10: (Top) Radial contraction during the simulated cycle for different points of the endocardium: base (black), equator (blue - -) and apex (red). (Bottom) Radial contraction extracted from tagged MRI by Philips Research France for different points of the myocardium.

real ones but also that the model has a good local behaviour.

5 Pathologies Simulation and Intervention Planning

Such a model enables the simulation of different pathologies, as well as the observation of the consequences of these pathologies on the simulated cardiac function.

Different electro-physiological disorders can be simulated, like a branch block or an ectopic focus. Then the action potential propagation can be simulated with these pathologies.

Most of the ventricular electro-physiological pathologies are not easily treated, and the radio-frequency ablation procedure is often lengthy, which results in considerable X ray doses delivered. Simulating the pathology and the outcome of different ablation strategies could help for the planning of such interventions.

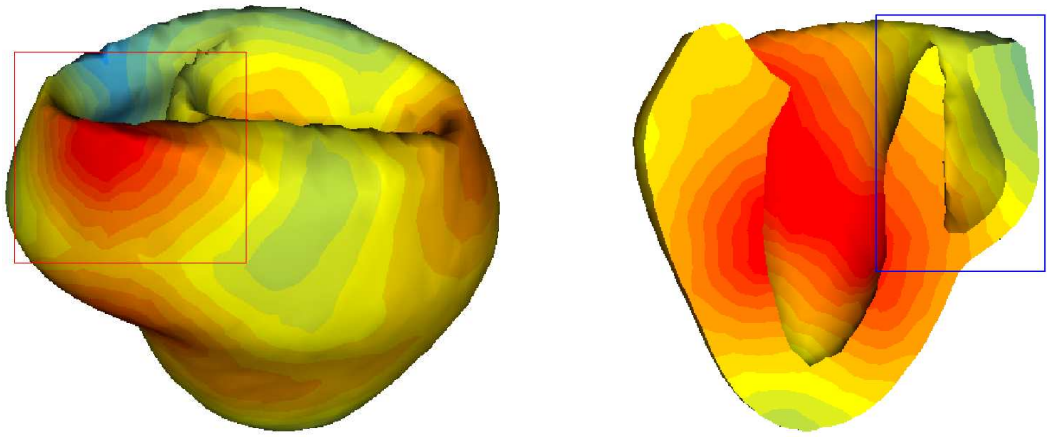

Figure 11: Electrophysiological pathologies simulation, resulting isochrones. (Left) Ectopic focus (part of a Wolff-Parkinson-White syndrome simulation). (Right) Right branch block simulation.

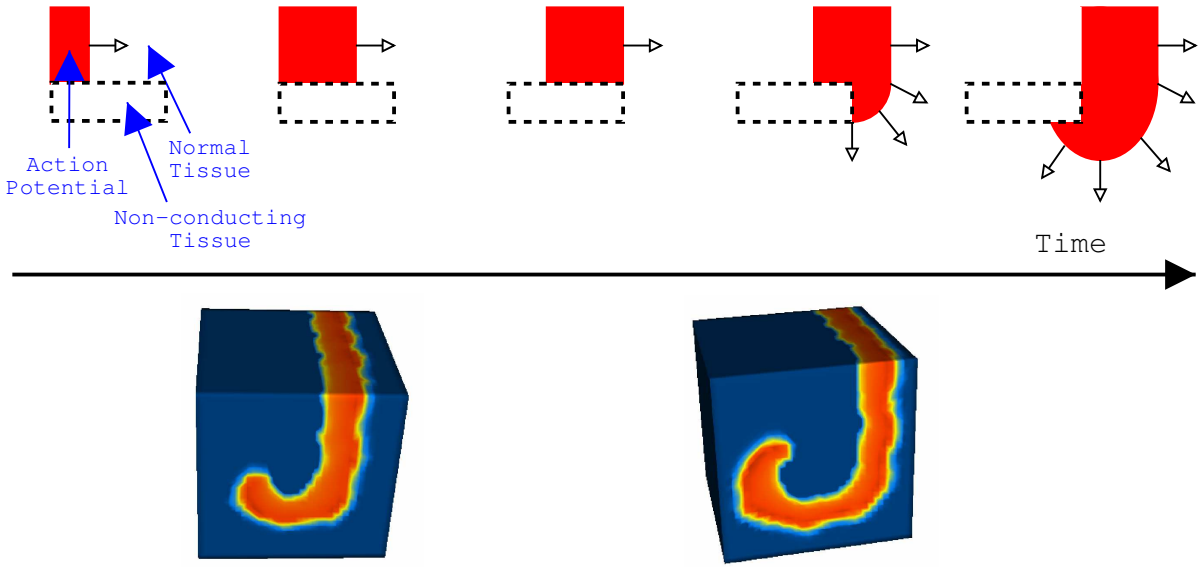

Figure 12: Simulation of a reentry spiral using a wave-break. (Top) Description of the wave-break method. (Bottom) Simulation on a cube of myocardium model. Colour represents the action potential (red: depolarised, blue: repolarised).

Moreover, some tissue pathologies, like infarcted areas, can be introduced in the potential propagation and in the mechanical contraction.

6 Pro-Active Deformable Model

Cardiac image segmentation is still a very active research area, due to the difficulty to propose a method robust to the variety of heart anatomy and imaging modalities as well as precise enough.

Many different approaches were proposed using models for cardiac image analysis [11]. In this overview, the proposed method would fit in continuous volumetric models.

One goal of this electromechanical model is to introduce prior knowledge on the cardiac

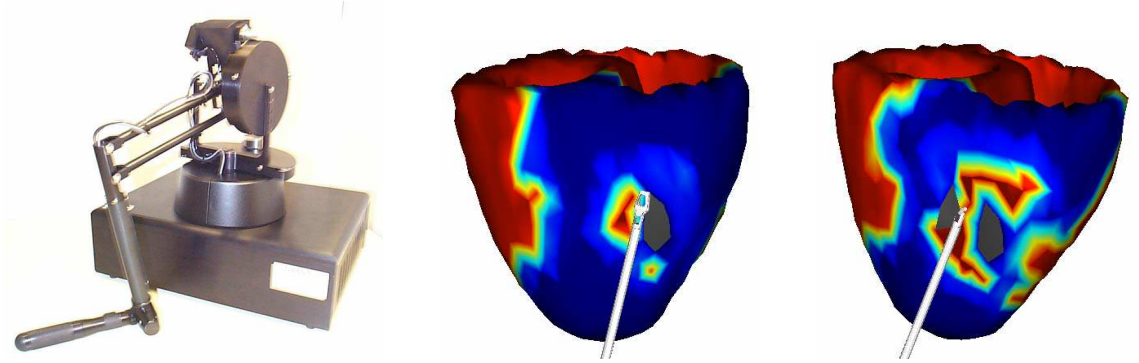

Figure 13: Phantom 3D interface, from Sensable Technologies and radio-frequency ablation simulation, by modifying the conducting parameters of the model, where it is in contact with the tool (black area).

motion in a medical image segmentation process. The idea is to use this model in the deformable model framework [23]. The internal energy regularising the deformation is computed from the electromechanical coupling and the external energy is computed from the image features.

Up to now, mainly deformable surfaces have been used [24]. Volumetric models have mainly been introduced for interpretation [29] or interpolation [9, 36, 3]. We believe that volumetric model also make possible to introduce much more *a priori* knowledge on the organ, as fibre direction and mechanical behaviour [28, 34].

Moreover, building a organ *in silico* also makes it possible to simulate the physiological behaviour of the organ, as the the action potential propagation, in order to introduce muscle contraction. This is what we call "Pro-Active Deformable Models".

6.1 External Energy

The external energy intervenes as external forces applied on the surface nodes of the model towards the closest image boundary voxel. This can be computed using criterions on the gradient value, the gradient direction, and the image region intensity.

These forces can be different on each of the different anatomical regions of the model, depending on what is visible in the image, and on the corresponding image region characteristics.

As the internal energy is volumetric, we have to control well the external energy to obtain a good balance. Another possibility is to also introduce volumetric external energy, using by example a block-matching approach [32].

6.1.1 Time-continuous Force Field

As we use a dynamic model for the internal energy, we need to integrate it according to a given time step, which is independent from the image acquisition time resolution. We create a "time-continuous force field" by using the two images of the sequence surrounding the current integrated time in the cycle, and we interpolate the force to apply from the two forces computed with each of these images.

6.2 Internal Energy

The internal energy is computed from the mechanical behaviour of the model and form the simulated contraction. The boundary conditions, like pressure and isovolumetric phases, are included in the image forces. And the added stiffness to represent the valves is also a part of the image forces. This is the reason why no boundary conditions other than image forces are applied when the model is used in this image analysis framework.

Due to the big difference in shape between the tele-diastolic position and the tele-systolic position, using *a priori* knowledge on the motion helps recover this deformation, as the image forces only have to correct the deformation, not create it from the tele-diastolic shape.

And the consequence is a better segmentation of the sequence, especially of the tele-systolic position (see fig. 14 and fig. 15).

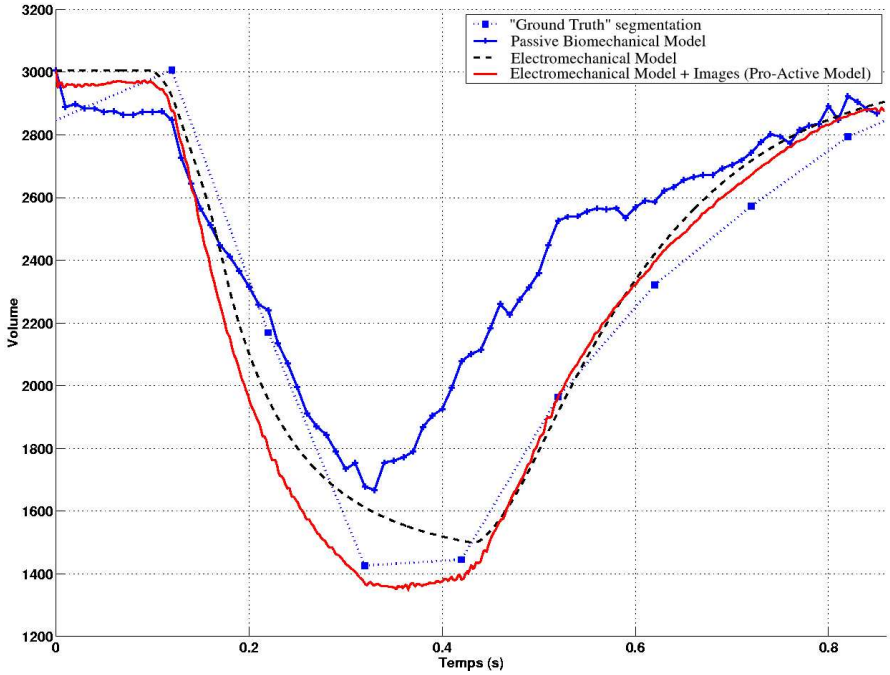

Figure 14: Comparison between the segmentation using the passive biomechanical model (blue line) and the pro-active model (red line). The ground truth segmentation (obtained using another method) is the blue squares, and the black dashed line shows the electromechanical model alone. The combined use of electromechanical model with image information makes possible a better segmentation.

Moreover, using this pro-active model gives *a priori* information on the local tangential motion (torsion) which is hardly visible in current medical images (without using tags). This kind of model could help recover this motion, which is quite important in cardiac function.

The segmentation of a sequence with the pro-active model takes less than 5 minutes on a standard PC, because we use a coarser mesh than for simulation, and the isovolumetric phases are not simulated.

7 Conclusion

This thesis proposes an electromechanical model of the heart designed for medical image analysis and simulation. This model has been validated on different global and local parameters

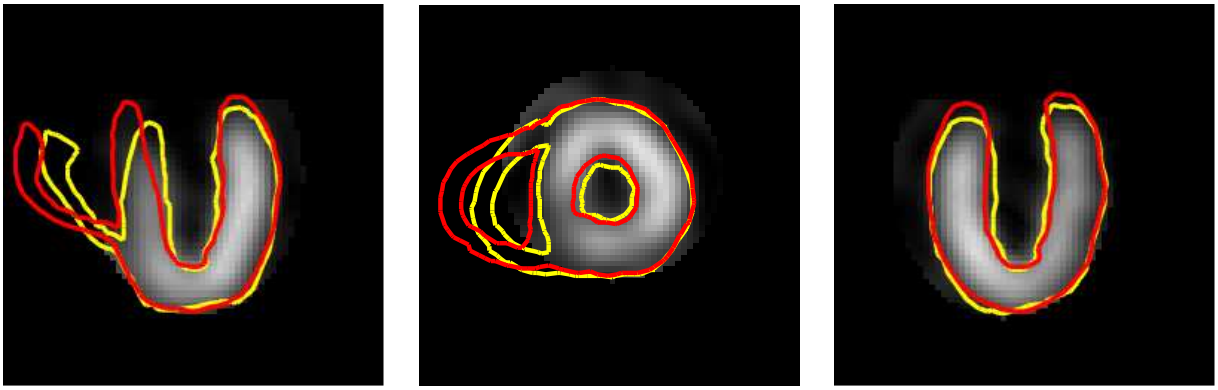

Figure 15: Comparison of the segmentation of a SPECT image sequence, in three orthogonal slices of the tele-systolic position (red: passive biomechanical model, yellow: pro-active model). The electromechanical model stays closer to the image boundary, especially near the base (axial contraction) and we can observe the right ventricle contraction of the model, even if the right ventricle is not visible in the image (due to a previous region of interest extraction).

of the cardiac function and then used for the segmentation of 4D medical image sequences.

We believe that such models can help the understanding of pathologies and the planning of different interventional strategies. Moreover, introducing *a priori* knowledge on the cardiac motion improves the segmentation of medical image sequences.

The long term aim is to use the model to devise less invasive techniques for electrophysiology studies that could transform the clinical applicability and effectiveness of these procedures. It can also help to estimate the cardiac function from clinical data, in order to better diagnose cardiovascular pathologies.

Current work include the validation of this model with experimental animal data [33] and with clinical patient data [31]. Translating model information into clinical practice requires novel functional imaging modalities for diagnosis, localisation and guided intervention. XMR interventional imaging, coupling x-rays and MR systems, can offer a good framework to achieve this goal [35].

The integration of models of human organs with biomedical imaging is a new research field that opens great possibilities in image analysis and medical simulation.

References

[1] R. Aliev and A. Panfilov. A simple two-variable model of cardiac excitation. *Chaos, Solitons & Fractals*, 7(3):293–301, 1996.

[2] C. Allouche, S. Makram, N. Ayache, and H. Delingette. A new kinetic modeling scheme for the human left ventricle wall motion with MR-tagging imaging. In *Functional Imaging and Modeling of the Heart (FIMH'01)*, number 2230 in Lecture Notes in Computer Science (LNCS), pages 61–68. Springer, 2001.

[3] F. Azar, D. Metaxas, and M. Schnall. Methods for modeling and predicting mechanical deformations of the breast under external perturbations. *Medical Image Analysis*, 6(1):1–27, 2002.

[4] G. W. Beeler and H. Reuter. Reconstruction of the action potential of ventricular myocardial fibers. *Journal of Physiology*, 268:177–210, 1977.

[5] J. Bestel, F. Clément, and M. Sorine. A biomechanical model of muscle contraction. In *Medical Image Computing and Computer-Assisted intervention (MICCAI'01)*, volume 2208 of *Lecture Notes in Computer Science (LNCS)*, pages 1159–1161. Springer, 2001.

[6] D. Caillerie, A. Mourad, and A. Raoult. Towards a fibre-based constitutive law for the myocardium. In *Modelling & Simulation for Computer-aided Medicine and Surgery (MS4CMS'02)*, 2002.

[7] D. Chapelle, F. Clément, F. Génot, P. Le Tallec, M. Sorine, and J. Urquiza. A physiologically-based model for the active cardiac muscle contraction. In *Functional Imaging and Modeling of the Heart (FIMH'01)*, number 2230 in Lecture Notes in Computer Science (LNCS), pages 128–133. Springer, 2001.

[8] D. Durrer, R. van Dam, G. Freud, M. Janse, F. Meijler, and R. Arzbaecher. Total excitation of the isolated human heart. *Circulation*, 41(6):899–912, 1970.

[9] M. Ferrant, A. Nabavi, B. Macq, , F. Jolesz, R. Kikinis, and S. Warfield. Registration of 3D intraoperative MR images of the brain using a finite element biomechanical model. *IEEE Transactions on Medical Imaging*, 20:1384–1397, 2001.

[10] R.A. FitzHugh. Impulses and physiological states in theoretical models of nerve membrane. *Biophysical Journal*, 1:445–466, 1961.

[11] A.F. Frangi, W.J. Niessen, and M.A. Viergever. Three-dimensional modeling for functional analysis of cardiac images: A review. *IEEE Transactions on Medical Imaging*, 1(20):2–25, 2001.

[12] J. Guccione and A. McCulloch. *Theory of Heart: biomechanics, biophysics, and nonlinear dynamics of cardiac function*, chapter Finite element modeling of ventricular mechanics, pages 121–144. Springer-Verlag, 1991.

[13] J. Häfner, F. Sachse, C. Sansour, G. Seemann, and O. Dössel. Hyperelastic description of elastomechanic properties of the heart: A new material law and its application. *Biomedizinische Technik*, 47-1/2:770–773, 2002.

[14] A. Hodgkin and A. Huxley. A quantitative description of membrane current and its application to conduction and excitation in nerve. *Journal of Physiology*, 177:500–544, 1952.

[15] E. Hsu and C. Henriquez. Myocardial fiber orientation mapping using reduced encoding diffusion tensor imaging. *Journal of Cardiovascular Magnetic Resonance*, 3:325–333, 2001.

[16] J. Humphrey, R. Strumpf, and F. Yin. Determination of a constitutive relation for passive myocardium: I. A new functional form. *ASME Journal of Biomechanical Engineering*, 112:333–339, 1990.

[17] P. Hunter, M. Nash, and G. Sands. *Computational Biology of the Heart*, chapter 12: Computational Electromechanics of the Heart, pages 345–407. John Wiley & Sons, 1997.

[18] P. Hunter and B. Smaill. The analysis of cardiac function: a continuum approach. *Biophysical molecular Biology*, 1988.

[19] Z. Knudsen, A.V. Holden, and J. Brindley. Qualitative modelling of mechano-electrical feedback in a ventricular cell. *Bulletin of mathematical biology*, 6(59):115–181, 1997.

[20] W.E. Lorensen and H.E. Cline. Marching cubes: a high resolution 3D surface reconstruction algorithm. *Computer Graphics (Proc. of SIGGRAPH)*, 21(4):163–169, 1987.

[21] C.H. Luo and Y. Rudy. A model of the ventricular cardiac action potential: depolarization, repolarization, and their interaction. *Circ. Res.*, 68:1501–1526, 1991.

[22] A. McCulloch, J.B. Bassingthwaighte, P.J. Hunter, D. Noble, T.L. Blundell, and T. Pawson. Computational biology of the heart: From structure to function. *Progress in Biophysics & Molecular Biology*, 69(2/3):151–559, 1998.

[23] T. McInerney and D. Terzopoulos. Deformable models in medical images analysis: a survey. *Medical Image Analysis*, 1(2):91–108, 1996.

[24] J. Montagnat and H. Delingette. A review of deformable surfaces: topology, geometry and deformation. *Image and Vision Computing*, 19(14):1023–1040, 2001.

[25] M. Nash. *Mechanics and Material Properties of the Heart using an Anatomically Accurate Mathematical Model*. PhD thesis, University of Auckland, 1998.

[26] P.M.F. Nielsen, I.J. Le Grice, B.H. Smail, and P.J. Hunter. Mathematical model of geometry and fibrous structure of the heart. *Am. J. of Physiol.*, 260(Heart Circ. Physiol. 29):1365–1378, 1991.

[27] D. Noble, A. Varghese, P. Kohl, and P. Noble. Improved guinea-pig ventricular cell model incorporating a diadic space, I_{Kr} and I_{Ks}, and length and tension dependent processes. *Canadian Journal of Cardiology*, 14:123–134, 1998.

[28] X. Papademetris, A. J. Sinusas, D. P. Dione, and J. S. Duncan. Estimation of 3D left ventricle deformation from echocardiography. *Medical Image Analysis*, 5(1):17–28, 2001.

[29] J. Park, D. Metaxas, and L. Axel. Analysis of left ventricular wall motion based on volumetric deformable models and MRI-SPAMM. *Medical Image Analysis*, pages 53–71, 1996.

[30] A. Pommert, K.-H. Höhne, B. Pflesser, E. Richter, M. Riemer, T. Schiemann, R. Schubert, U. Schumacher, and U. Tiede. Creating a high-resolution spatial/symbolic model of the inner organs based on the visible human. *Medical Image Analysis*, 5(3):221–228, 2001.

[31] K. Rhode, M. Sermesant, G. Sanchez-Ortiz, S. Hegde, D. Rueckert, D. Hill, and R. Razavi. XMR guided cardiac electrophysiology study and radio frequency ablation. In A. Amini, editor, *SPIE Medical Imaging*, 2004.

[32] M. Sermesant, O. Clatz, Z. Li, S. Lantéri, H. Delingette, and N. Ayache. Parallel implementation of volumetric biomechanical model and block-matching for fast non-rigid registration. In *International Workshop on Biomedical Image Registration (WBIR'03)*, number 2717 in Lecture Notes in Computer Science (LNCS), pages 398–407. Springer, 2003.

[33] M. Sermesant, O. Faris, F. Evans, E. McVeigh, Y. Coudière, H. Delingette, and N. Ayache. Preliminary validation using *in vivo* measures of a macroscopic electrical model of the heart. In *International Symposium on Surgery Simulation and Soft Tissue Modeling (IS4TM'03)*, 2003.

[34] M. Sermesant, C. Forest, X. Pennec, H. Delingette, and N. Ayache. Deformable biomechanical models: Application to 4D cardiac image analysis. *Medical Image Analysis*, 7(4):475–488, 2003.

[35] M. Sermesant, K. Rhode, S. Hegde, G. Sanchez-Ortiz, D. Rueckert, P. Lambiase, C. Bucknall, D. Hill, and R. Razavi. Modelling the cardiac electromechanical activity for integration of electrophysiological studies with MR. In *Society for Cardiovascular Magnetic Resonance Scientific Sessions*, 2004. to appear.

[36] O. Skrinjar. *Deformable Models in Image-Guided Neurosurgery.* PhD thesis, Yale University, 2002.